BYG DTU

# A Composite Theory
## as related to materials design

Lauge Fuglsang Nielsen

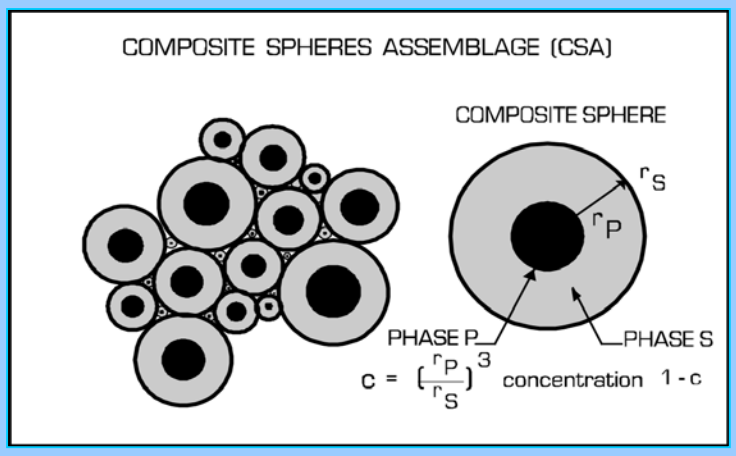


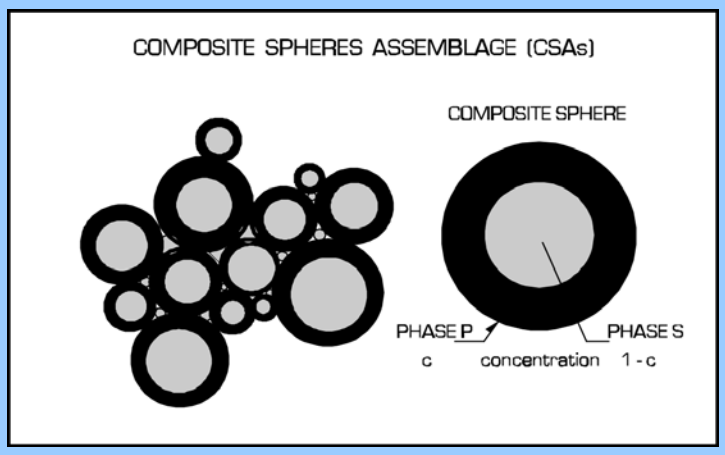


DANMARKS
TEKNISKE
UNIVERSITET

Rapport
BYG•DTU R-078
October 2003
ISSN 1601-2917
ISBN 87-7877-141-2

# A Composite Theory
## *as related to materials design*

Lauge Fuglsang Nielsen

**Abstract:** An operational summary of a composite theory previously developed by the author is presented in this paper. The theory differs from other composite theories by predicting 'global' property solutions, which are valid for any composite geometry. Properties looked at are mechanical, such as stiffness, eigenstrain/stress (e.g. shrinkage and thermal expansion), and physical, such as various conductivities with respect to heat, electricity, and chlorides.

'Local' property solutions applying for specific composites are obtained from the global solutions introducing geometry specific, so-called shape functions. Examples are presented, demonstrating a very satisfying agreement between material properties determined experimentally and such properties predicted by the theory considered.

In a special section of the paper the theory is examined with respect to its potential with respect to materials design. Examples are presented, demonstrating how the method can be inversed to determine types of composite geometry from prescribed composite properties, such as Young's moduli and conductivities. Research projects are suggested by which new production techniques might be found which are more rational than the ones known to day.

A software, 'CompDesign' is prepared with application programs covering both the prediction aspects and the design aspects of the method presented. On special request the software is available contacting the author, lfn@byg.dtu.dk

# 1. INTRODUCTION

The present paper is based on a composite theory for isotropic composite materials originally suggested by the author in (1), and further developed in (2,3,4). Contrary to other composite theories, 'global' solutions (Equations 7-11) are predicted by this theory, which are valid for any composite geometry. Geometry in general is represented by so-called geo-functions ($\theta$).

'Local' solutions applying for composites with specific geometries are subsequently obtained introducing geometry dependent, so-called shape functions ($\mu$) into these geo-functions. The shape functions are the same whether stiffness or conductivity related problems are considered.

The 'global' feature of the theory means that it has a potential with respect to materials design. In order to study this potential more closely, an operational summary of a simplified version of the author's theory, as reported in (4), is presented in the first part of this paper.

Some preliminary studies on materials design are then made in the second part of the paper with suggestions made on further research in the field of materials design, theoretical, numerical, as well as experimental. A software, 'CompDesign' has been prepared

with application programs covering both the prediction aspects and the design aspects of the method presented. On special request the software is available contacting the author, lfn@byg.dtu.dk

## 1.2 General conditions

The composites considered are isotropic mixtures of two components: phase P and phase S. The amount of phase P in phase S is quantified by the so-called volume concentration defined by $c = V_P/(V_P+V_S)$ where volume is denoted by V. It is assumed that both phases exhibit linearity between response and gradient of potentials, which they are subjected to. For example: Mechanical stress versus deformation (Hooke's law), heat flow versus temperature, flow of electricity versus electric potential, and diffusion of a substance versus concentration of substance.

The composite properties specifically considered are stiffness, eigenstrain (such as shrinkage and thermal expansion), and various conductivities (with respect to chloride or heat flow e.g.) as related to volume concentration, composite geometry, and phase properties: Young's moduli $E_P$ and $E_S$ with stiffness ratio $n = E_P/E_S$, eigenstrains $\lambda_P$ and $\lambda_S$, and conductivities $Q_P$ and $Q_S$ with conductivity ratio $n_Q = Q_P/Q_S$. Further notations used in the text are explained in the list of notations at the end of the paper.

In general the following assumptions are introduced in this paper:

- For simplicity (but also to reflect most composite problems encountered in practice) stiffness and stress results presented assume an elastic phase behavior with Poisson's ratios $\nu = 0.2$ (in practice $\nu \approx 0.2$). This means that, whenever stiffness and stress expressions are presented, they can be considered as generalized quantities, applying for any loading mode: shear, volumetric, as well as uni-axial. For example, $E/E_S$ can also be used to predict the composite shear modulus, $G/G_S$, and the composite bulk modulus, $K/K_S$, normalized with respect to the phase S properties. In a similar way the phase stresses, $\sigma_P/\sigma$ and $\sigma_S/\sigma$, also apply independently of loading mode as long as both phase stress modes ($\sigma_P$,$\sigma_S$) and composite (external) stress modes ($\sigma$) are the same. (It is noticed that phase stress and phase strain are defined by their respective volume averages in phase considered).

Not to exaggerate our present knowledge of composite geometries it has, deliberately, been chosen to keep geometry described by simple mathematical expressions.

Typographically, the author's general theory (as presented in 4) is simplified very much by these assumptions: Only the volumetric analysis, for example, has to be considered - and the tensor notation can be dropped.

# 2. GEOMETRY

Geometries in a composite change as the result of volume transformations associated with increasing phase P concentration. We will think of changes as they are stylized in Figure 1: At increasing concentration, from $c = 0$, discrete phase P elements agglomerate and change their shapes approaching a state at the so-called critical concentration, $c = c_S$, where they start forming continuous geometries. Phase P grows fully continuous between $c = c_S$ and the second critical concentration, $c = c_P \geq c_S$ such that the composite geometry from the latter concentration has become a mixture of discrete, de-agglomerating, phase S particles in a continuous phase P.

At fixed concentrations the following terminology is attached to the various stages of geometry changes just explained: DC means a discrete phase P in a continuous phase S. MM means a mixed phase P geometry in a mixed phase S geometry, while CD means a continuous phase P mixed with a discrete phase S. We notice that MM-geometries (if porous) are partly impregnable. In modern terminology this means that phase P percolation exists in composites with $c > c_S$. Percolation is complete for $c \geq c_P$. Porous materials have lost any coherence in this concentration area with no stiffness and strength left.

In a complementary way the geometry history of phase S follows the history of phase P and vice versa. Formally the geometries explained above can be shifted along the concentration axis. A composite may develop from having a DC geometry at c = 0 to having a MM geometry at c = 1. Such composite geometries, with $c_P > 1$ and $0 < c_S < 1$, are named DC-MM geometries. Other composites may keep their DC type of geometry all the way up to c = 1 in which case the composite geometry is denoted as a DC-DC geometry, with both critical concentrations > 1. The geometry outlined in Figure 1 changes from DC to CD geometry which makes it a DC-CD geometry with both critical concentrations in c = 0-1.

We notice that critical concentrations can be fictitious (outside c = 0 - 1). In such cases they do not, of course, have the immediate physical meanings explained above. Formally, however, we keep this 'explanation' in order to describe in an easy way, how the rate of changing the composite geometry is influenced by the processing technique used. The description of composite geometry can be summarized as explained in Figure 1 with so-called shape functions, $\mu_P \leq 1$ and $\mu_S \leq 1$, subsequently explained in more details.

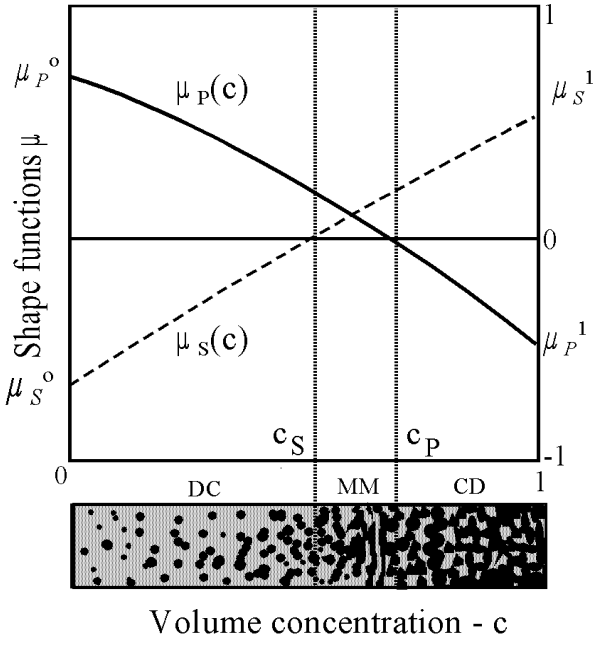


***Figure 1.*** *Geometrical significance of shape functions: $(\mu_P,\mu_S)$ = (+,-) means a discrete phase P in a continuous phase S. $(\mu_P,\mu_S)$ = (+,+) means that both phases P and S appear with a mixed geometry. $(\mu_P,\mu_S)$ = (-,+) means a continuous phase P mixed with discrete phase S elements. Black and gray signatures denote phase P and phase S respectively. $(\mu_P^o,\mu_S^o,\mu_P^1,\mu_S^1)$ are so-called shape factors. $(c_P,c_S)$ are so-called critical concentrations.*

Ideal geometries at c = 0 and at c = 1 of a DC-CD composite are illustrated in Figures 2 and 3 respectively. We notice in this context that the composite theory developed by the author is based on the concept that any isotropic composite geometry is a station on a geopath moving *from the CSA$_P$ geometry shown in Figure 2 to the CSA$_S$ geometry shown in Figure 3.* (CSA is an abbreviation for the composite model, Composite Spheres Assemblage, introduced by Hashin in (5)).

**Remarks:** It is noticed that the four letter symbols for composite geometries are subsequently also used in the meaning, for example: a 'DC-CD type of composite', a 'DC-CD type of geometry', or just a 'DC-CD composite'.

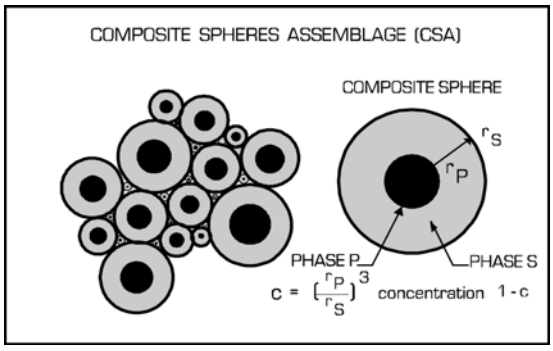


***Figure 2.*** *Composite spherical assemblage with phase P particles, $CSA_P$.*

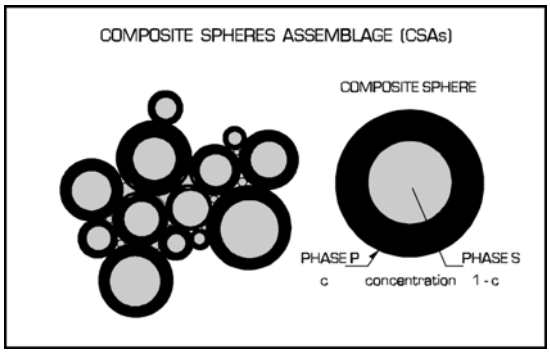


***Figure 3.*** *Composite Spheres Assemblage with phase S particles, $CSA_S$.*

## 2.1 Types of geometry

In general, flexible phase geometries are considered which can adjust them selves to form a tight composite. The adjustment can be natural (as in normal concretes with moderate aggregate concentrations), or organic (as in bone structures), or it can be the result of a melting process, or compaction (as in sintered powder composites).

The various types of geometries considered in this paper are listed in Figure 4: *Particulate composites* are defined by the former row. They have particles in a matrix geometry (DC) at small concentrations. *Lamella composites* are defined by the latter row. They have a mixed phase P geometry in a mixed phase S geometry (MM) at low concentrations. Obviously, the phenomenon of percolation previously considered develops between the two critical concentrations. In Figure 4 gray shadings indicate the phase P percolation previously considered. We assume that percolation varies linearly from being 0 at $c < c_S$ to being 100% at $c > c_P$.

Examples of the composites outlined in Figure 4 are presented in Table 1.

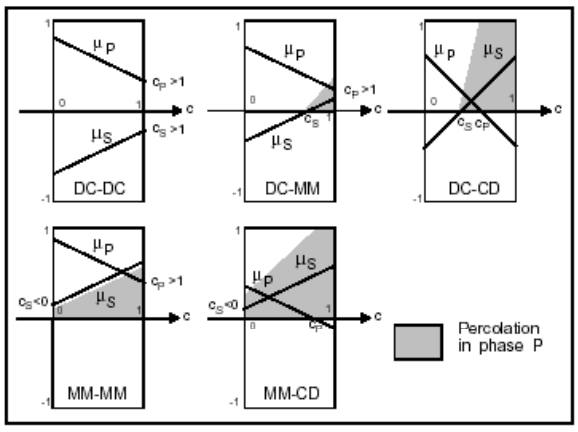


***Figure 4.*** *Composite types versus critical concentrations. Former and latter two letters denote composite geometry at c = 0 and at c = 1 respectively.*

**Remark**: Important exceptions from the geometry types indicated above can also be considered by the theory presented in this paper: Particulate composites with self-inflicted po-

res, such as light clinker concrete and other lean concretes with a deficit of mortar (phase S). Such materials can be analysed with shape functions $(\mu_P,\mu_S) \equiv (\mu_P(c_S),0)$ for $c \geq c_S$, considering composite geometry to be 'frozen' at $c = c_S$ approximated to be that concentration where particles start to interfere forming a stable continuous[1] skeleton – and where phase S starts becoming porous (only way to increase phase P concentration). In details a composite analysis of particulate materials with self-inflicted pores is made in (4). In the present work we will limit our selves only to show some results from such analysis in Section 5.3.

# 3. SHAPE FUNCTIONS (a closer look)

As previously mentioned, shape functions define the type of composite geometry as it develops when the volume concentration of phase P increases from c = 0 to c = 1. Obviously this 'history' is very much a matter of production technology, which cannot be studied by theoretical means only. Reasonable estimates, however, can be made (4) with broken-line descriptions from knowing about shape factors (shape function values at c = 0 and at c = 1, $\mu_P^o,\mu_S^o,\mu_P^1,\mu_S^1$) and from knowing about critical concentrations ($c_P$ and $c_S \leq c_P$, where one shape function value is 0).

In this section we will present information, which are just enough to construct reliable shape functions from:

- Shape factors which tell about the shapes of phase components at their respective dilute concentrations, and from
- Critical concentrations, which tell, where the composite geometry changes from one type to another type.

| TYPE | | EXAMPLES |
|---|---|---|
| **DC** | **DC** | Particulate composite (concrete, mortar). Extremely high quality of grading (approaching $CSA_P$ composites).<br>*Pore system:* Not impregnable. Finite stiffness at any porosity |
| | **MM** | Particulate composite (concrete, mortar) with particle interference at $c = c_S$. Increasing quality of grading is quantified by larger concentration $c_S$ at first severe interference.<br>*Pore system:* Only impregnable for porosities $c > c_S$. Finite stiffness at any porosity. |
| | **CD** | Mixed powders (ceramics).<br>*Pore system:* Only impregnable for porosities $c > c_S$. No stiffness for porosities $c > c_P$. |
| **MM** | **MM** | Mixed lamella/foils ("3D-plywood").<br>*Pore system:* Fully open at any porosity. Finite stiffness at any porosity. |
| | **CD** | Mixed lamella/foils ("3D-plywood").<br>*Pore system:* Fully open at any porosity. No stiffness for porosities $c > c_P$. |

***Table 1.*** *Examples of composites outlined in Figure 4.*

## *3.1 Shape factors*

For particulate composites (DC) with phase P being a mixture of uni-shaped ellipsoidal particles in a continuous phase S, shape factors can be estimated by the following expressions reproduced from (4),

[1] We simulate particles to agglomerate by a thin, 'sufficiently' strong phase S glue.

$$\mu_P^o = \begin{cases} \dfrac{3A}{A^2 + A + 1} & ; A \le 1 \\ 3\,\dfrac{A^2 - A + 1}{4A^2 - 5A + 4} & ; A > 1 \end{cases} \quad ; \quad \mu_S^o = - \begin{cases} \mu_P^o & ; A \le 1 \\ 4\,\mu_P^o - 3 & ; A > 1 \end{cases} \quad in\ DC \qquad (1)$$

where A is the so-called aspect ratio, A = length/diameter of P-particles. Spherical particles have A = 1. Long particles have A > 1. Flat particles have A < 1.

In a similar way shape factors for particulate composites (CD) with phase S being a mixture of uni-shaped ellipsoidal particles in a continuous phase P can be estimated by the following expressions, where $A_S$ is now the aspect ratio of S particles.

$$\mu_S^1 = \begin{cases} \dfrac{3A_S}{A_S^2 + A_S + 1} & ; A_S \le 1 \\ 3\,\dfrac{A_S^2 - A_S + 1}{4A_S^2 - 5A_S + 4} & ; A_S > 1 \end{cases} \quad ; \quad \mu_P^1 = - \begin{cases} \mu_S^1 & ; A_S \le 1 \\ 4\,\mu_S^1 - 3 & ; A_S > 1 \end{cases} \quad in\ CD \qquad (2)$$

The uni-shape shape factors presented are generalized in (4) to include arbitrary particle shape distributions. For the case of mixtures with only two aspect ratios, shape factors are automatically determined by the software 'CompDesign' previously referred to: An example: shape factors ($\mu_P^o$,$\mu_S^o$) = (0.83,-0.68) are the results of mixing 20% A = 0.3 with 80% A = 2.

Shape factors for laminate composites (MM) cannot be calculated as easily as for CD and DC composites. Some guidelines for estimates are presented in (4) calibrated from FEM analysis of MM-MM composites reported in (1,4). In the present context we may estimate shape factors directly from Figure 5 discussed in subsequent Section 3.3.

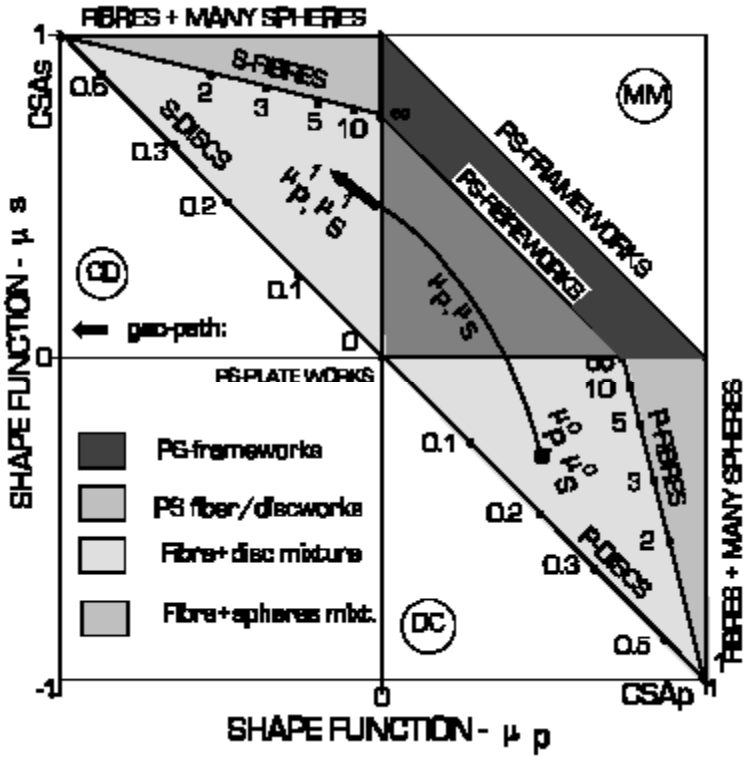


***Figure 5.*** *Geo-path and description of geometries: Numbers in section DC indicate aspect ratios A = length/diameter of phase P particles. Corresponding aspect ratios of S particles are presented in section CD.*
*Frame- and fiber works are agglomerating MM-structures of long crumbled fibers and shorter crumbled fibers respectively. Fiber/disc works are agglomerating MM-structures of crumbled fibers and discs. Plate works are agglomerating crumbled discs (sheets/foils).*
*The critical concentrations $c_P$ and $c_S$ correspond to $\mu_P = 0$ and $\mu_S = 0$ respectively.*

## *3.2 Critical concentrations*

It is emphasized that the critical concentrations depend very much on the processing technique used to produce composites. We notice that particle size distribution is part of processing. For particulate composites, for example, the critical concentration $c_S$ can be thought of as the concentration at first interference of phase P (starting to create a continuous skeleton). Improved quality of size distribution (smoothness and density) is considered by increasing $c_S$. At this concentration porous materials become very stiff when impregnated with a very stiff material. At the other critical concentration, $c_P > c_S$, the composite becomes a mixture of phase S elements completely wrapped in a matrix of phase P. Porous materials loose their stiffness and strength at $c_P$ because phase P has become a continuous, enveloping, void system.

As previously indicated, critical concentrations can be fictitious (outside c = 0 - 1). In such cases critical concentrations will have to be estimated from experience, or detected from calibration experiments.

## *3. 3 Path of geometry*

According to (4) the geo-path graph outlined in Figure 5 is a convenient way of describing the types of geometries traversed when volume concentrations for a specific composite proceed from c = 0 to c = 1 ($\mu_P$ goes from $\mu_P^o$ to $\mu_P^1$ and $\mu_S$ goes from $\mu_S^o$ to $\mu_S^1$).

### 3.3.1 Present analysis

In the present analysis we simplify the description of composite geometry by introducing the straight-line geo-path shown in Figure 6. Mathematically the path is described as follows with a so-called path factor, $0 \le a \le 1$,

$$\mu_S = a - \mu_P; \quad with \quad path \quad factor \quad a = \mu_P^o + \mu_S^o \tag{3}$$

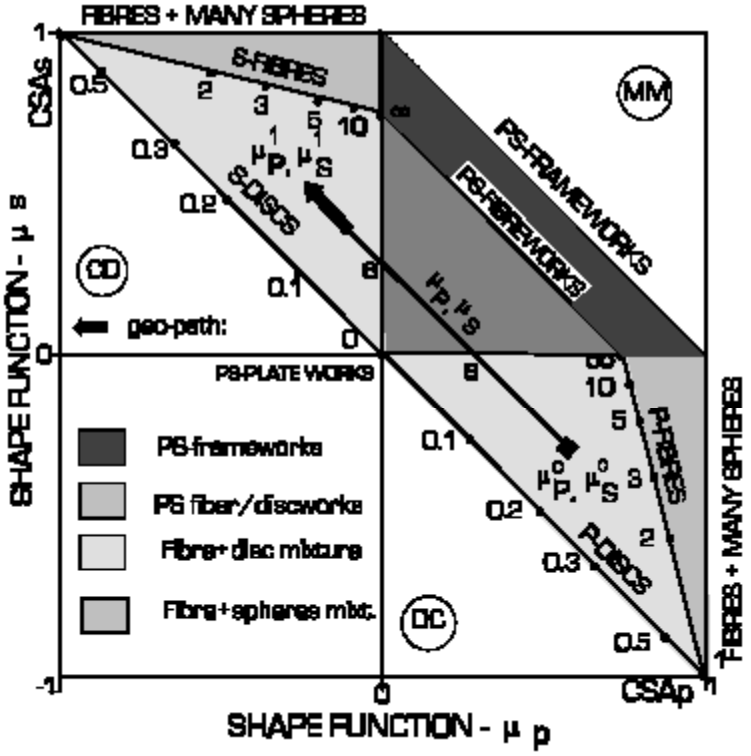


***Figure 6.*** *Present analysis: Simplified geo-path and description of geometries according to Equation 3. Shape functions 'predicted' are presented in Equation 4.*

The shape functions associated (see Figure 1, with linear graphs) are related as follows,

$$\mu_P = \mu_P^o\left(1 - \frac{c}{c_P}\right) \;;\; \mu_S = \mathrm{MIN}\begin{pmatrix} \mu_S^o\left(1 - c/c_S\right) \\ 1 \end{pmatrix} \quad with \quad c_P = -c_S\,\frac{\mu_P^o}{\mu_S^o} \tag{4}$$

It is recognized that these shape functions are determined by only three geo-parameters, for example two shape factors ($\mu_P^o$,$\mu_S^o$) and one critical concentration ($c_P$ or $c_S$). As a consequence, the other three geo-parameters are 'predicted'. Despite this deficiency, it is demonstrated in (4,17) that Equation 4 is a successful basis for a number of composite analysis on composites made with traditional technologies: Particles mixed into a continuous matrix, compaction of powders, production of porous materials, impregnation of porous materials, and three dimensional 'Plywood' (composite made of mixed crumbled P and S lamella/foils).

In general, however, we must be prepared to work with more complex geo-paths $\mu_S = f(\mu_P)$ adapted more accurately to production technology used. A discussion on this feature has been made in (4). Future research on this important feature is outlined at the end of this paper.

# 4. COMPOSITE ANALYSIS

## 4.1 Global solutions

As previously mentioned, the author's theory predicts global solutions for composite problems. Examples are presented in Equations 7-11 with symbols explained in the list of notations at the end of this paper. The influence of geometry on these solutions is 'hidden' in the following so-called geo-functions developed in (4),

*Geo - function for stiffness analysis :*

$$\theta = \frac{1}{2}\left[\mu_P + n\mu_S + \sqrt{(\mu_P + n\mu_S)^2 + 4n(1 - \mu_P - \mu_S)}\right] \;;\; n = \frac{E_P}{E_S} \tag{5}$$

*Geo - function for conductivity analysis :*

$$\theta_Q = \mu_P + n_Q\mu_S + \sqrt{(\mu_P + n_Q\mu_S)^2 + 4n_Q(1 - \mu_P - \mu_S)} \;;\; n_Q = \frac{Q_P}{Q_S} \tag{6}$$

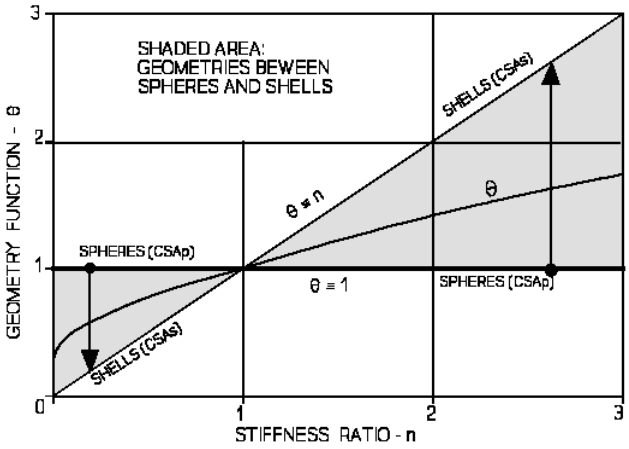


***Figure 7.*** *Influence of phase P geometry on the stiffness geo-function θ. Phase P being spheres in a continuous phase S ($CSA_P$) is defined by $\theta \equiv 1$. Phase S being spheres in a continuous phase P ($CSA_S$) is defined by $\theta \equiv n$. Composites with geometries between these extremes have θ in shaded area. For the conductivity geo-function, $\theta_Q$, the shaded area is bounded by $\theta_Q \equiv 2$ (for $CSA_P$) and $\theta_Q \equiv 2n_Q$ (for $CSA_S$)*

A geo-function looks as shown in Figure 7. In general, specific composite geometries are 'mapped' by the shape functions ($\mu_P$,$\mu_S$) previously considered in Section 3 (with six geo-parameters: Four shape factors ($\mu_P^o$,$\mu_S^o$, $\mu_P^1$,$\mu_S^1$) and two critical concentrations ($c_P$,$c_S$)).

**Remark:** We re-call from the introduction that the stiffness- and stress expressions presented have generalized meanings. They can be used for any loading mode, shear, volumetric, as well as uni-axial. We also re-call that stress and strain are volume averages.

*Stiffness :*

$$e = \frac{E}{E_S} = \frac{n + \theta\,[1 + c(n-1)]}{n + \theta - c(n-1)} = \frac{1 - c}{1 + c/\mu_P} \quad if\ porous \quad (\equiv 0\ if\ c \geq c_P) \tag{7}$$

*Stress due to external load*

$$\frac{\sigma_P}{\sigma} = \frac{n(1+\theta)}{n + \theta\,[1 + c(n-1)]} \;;\; \frac{\sigma_S}{\sigma} = \frac{n + \theta}{n + \theta\,[1 + c(n-1)]} \tag{8}$$

*Eigenstrain (linear)*

$$\lambda = \lambda_S + \Delta\lambda\,\frac{1/e - 1}{1/n - 1} \;;\quad (\Delta\lambda = \lambda_P - \lambda_S) \tag{9}$$

*Eigenstress (hydrostatic)*

$$\rho_P = -\frac{5}{3} E_S \Delta\lambda\,\frac{c(1/n-1) - (1/e-1)}{c(1/n-1)^2} \;;\; \rho_S = -\frac{c}{1-c}\rho_P \tag{10}$$

*Conductivity :*

$$q = \frac{Q}{Q_S} = \frac{n_Q + \theta_Q\,[1 + c(n_Q - 1)]}{n_Q + \theta_Q - c(n_Q - 1)} = \frac{1 - c}{1 + c/(2\mu_P)} \quad if\ porous \quad (\equiv 0\ if\ c \geq c_P) \tag{11}$$

## 4.2 Local solutions

As already indicated, the global composite solutions just presented are easily converted to local solutions for specific composite materials. We only have to introduce the corresponding shape functions, $\mu_P$,$\mu_S$, into the geo-functions, $\theta$ ($\theta_Q$). Examples of various composite analyses are presented in the subsequent Section 5.

### *Bounds on stiffness and conductivity*

The stiffness- and conductivity predictions are bounded as follows between the exact solutions for the CSA composites illustrated in Figures 2 and 3.

*Stiffness bounds*

$$\frac{n + 1 + c(n-1)}{n + 1 - c(n-1)} \leq e = \frac{E}{E_S} < n\,\frac{2 + c(n-1)}{2n - c(n-1)} \tag{12}$$

*valid for $n \geq 1$; reverse signs when $n < 1$*

*Conductivi ty bounds*

$$\frac{n_Q + 2[1 + c(n_Q - 1)]}{n_Q + 2 - c(n_Q - 1)} \le q = \frac{Q}{Q_S} \le n_Q \frac{3 + 2c(n_Q - 1)}{3n_Q - c(n_Q - 1)} \qquad (13)$$

*valid for* $n_Q \ge 1$ *; reverse signs when* $n_Q < 1$

The former bounds are obtained from Equation 7 introducing $\theta \equiv 1$ and $\theta \equiv n$ respectively. The latter bounds are obtained from Equation 11 introducing $\theta_Q \equiv 2$ and $\theta_Q \equiv 2n_Q$ respectively, see legend to Figure 7. The bounds such determined are the same as can be obtained from the studies made by Hashin and Shtrikman in (6) on composite stiffness and in (7) on composite conductivity. The bounds are subsequently referred to by H/S.

# 5. EXAMPLES

Two examples are presented in this section where composites are subjected to a property analysis exactly as outlined in this paper with shape functions expressed by Equation 4.

To verify the statement previously made that a composite analysis of particulate composites with self-inflicted pores (which are in fact porous two-phase composites) can, in principles, also be made by the theory presented in this paper, some results from a composite analysis made in (4) are reproduced in Section 5.3.

## 5.1 Thermal expansion of salt infected bricks

The dotted data shown in Figure 8 are from an experimental study reported in (8) on damage of bricks caused by salt intrusion. The solid line data are the results of a composite analysis with the following component properties reproduced from (4). Additional results from the analysis are the internal stresses presented in Figure 9.

Composite: CC-CD with $(\mu_P^o, c_P) = (0.9, 0.53)$ and estimated $\mu_S^o = 0.05$

Phase S (Tile): $E_S = 38000$ MPa, $\lambda_S = 6*10^{-6}/^oC$

Phase P (Salt): $E_P = 20000*\beta/(2-\beta)$ MPa, (degree of pore impregnation: $\beta$ = vol impregnated/total pore vol = 0.15 - 0.25)

$\lambda_P = 3.8*10^{-5}/^oC$

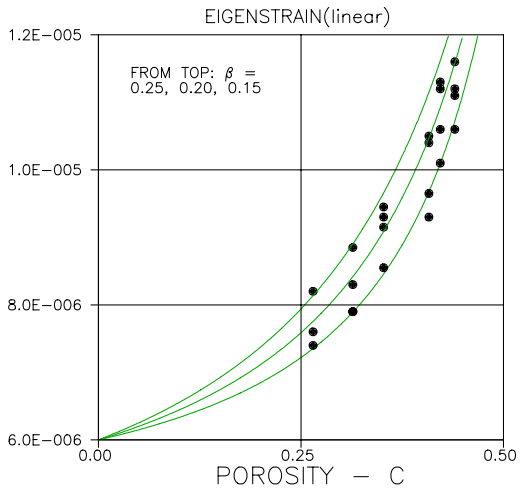


***Figure 8.*** *Thermal eigenstrain (/°C) of salt infected tile.*

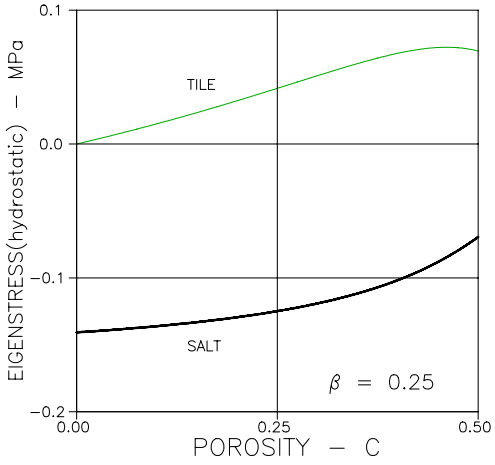


***Figure 9.*** *Predicted thermal eigenstresses (/°C) in salt infected brick*

The reduction of the phase P Young's modulus is due to the fact observed in (8) that the solidification of salt – due to shrinkage - was effective in only $\beta = 15 – 25$ % of the pore volume available. (By the reduction factor used above, phase P is homogenized to be a porous $CSA_P$ material). Eigenstrain ($\lambda$) is not influenced by porosity.

## 5.2 Stiffness and Chloride diffusion in cement paste system

A stiffness- and a conductivity analysis is now made on a cement paste system with the following phase- and geometrical properties:

*Phase properties:* The components are phases (P,S) = (saturated capillary pores, cement gel). The Young's moduli and the Chloride diffusion coefficients are ($E_P$, $E_S$) = (0,32000) MPa and ($Q_P$,$Q_S$)/$Q_P$ = (1, 0.00008) respectively (with $Q_P = 2*10^{-9}$ $m^2$/sec). These data are deduced from stiffness experiments reported in (9,10) and from chloride diffusion experiments reported in (11,12).

*Geometry:* We estimate that pores, at an average, have an aspect ratio of A = 4 at low porosities. Shape factors of ($\mu_P^o$,$\mu_S^o$) = (0.81,-0.25) are then calculated by Equation 1. A critical concentration of $c_P = 0.78$ is estimated from (13) where it was shown that cement paste exhibits no stiffness (and strength) at porosities greater than $c \approx 0.78$. (The solid phase (S) becomes surrounded by voids at that concentration). From Equation 4 we get $c_S = 0.24$.

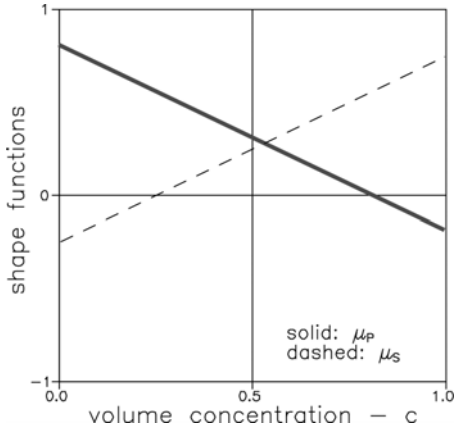


***Figure 10.*** *Geometry of cement paste considered. c is cap-porosity.*

*Analysis:* Shape functions are now determined by Equation 4 as presented in Figure 10. A composite analysis proceeds exactly as explained in the previous sections of the paper. The results are shown in Figures 11 and 12 together with the respective test data.

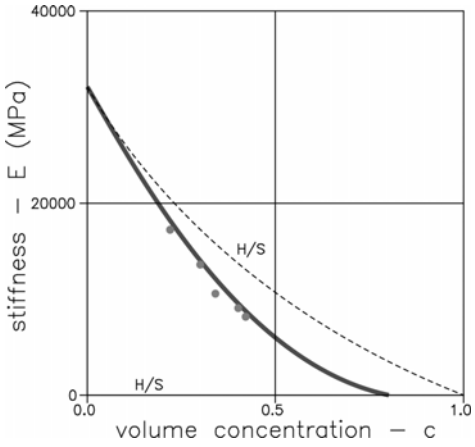


***Figure 11.*** *Cement paste system considered: Stiffness as related to capillary - porosity (c), present analysis.*

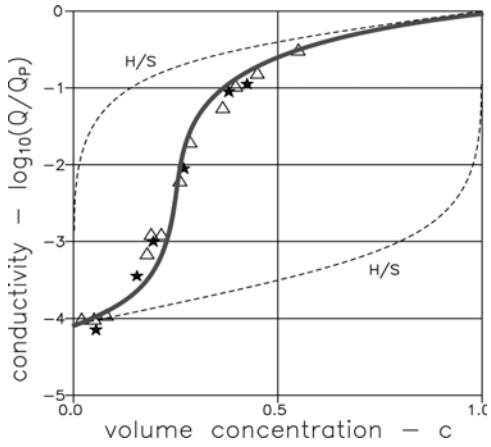


***Figure 12.*** *Cement paste system considered: Chloride diffusivity as related to capillary porosity (c), present analysis.*

### *5.2.1 Alternative geometries*

It is of some interest to compare the results just obtained with predictions based on well-known, traditional composite geometries:

1) *DC-CD composite made of a compacted mixture of P and S spheres:* (In the present theory quantified by $(A,c_S) = (1,0.5) \Rightarrow \mu_P = 1 - 2c$ and $\mu_S = 2c - 1$). The stiffness prediction for this geometry can be presented in a closed analytical form, namely Equation 14, which according to (1), is identical to a solution, that can be obtained from the theoretical analysis of particulate composites made by Budiansky (14).

$$e = \frac{1}{2}\left[ (1-n)(1-2c) + \sqrt{(1-n)^2(1-2c)^2 + 4n} \right] \quad (Budiansky) \tag{14}$$

2) *DC-DC composite with P-spheres in a continuous S-matrix, see Figure 2:* (In the present theory quantified by $(A,c_S) = (1,\infty) \Rightarrow \mu_P \equiv 1$ and $\mu_S \equiv -1$). The stiffness prediction for this geometry can also be given a closed analytical form, namely Equation 12(left side) which is identical to the $CSA_P$ solution previously referred to by Hashin (5) – corresponding to one of the H/S bounds.

We notice from Figures 11 - 14 that the influence of composite geometries 1) and 2) on composite properties are very different from the influence of the geometry applying for the composite system originally considered in this example.

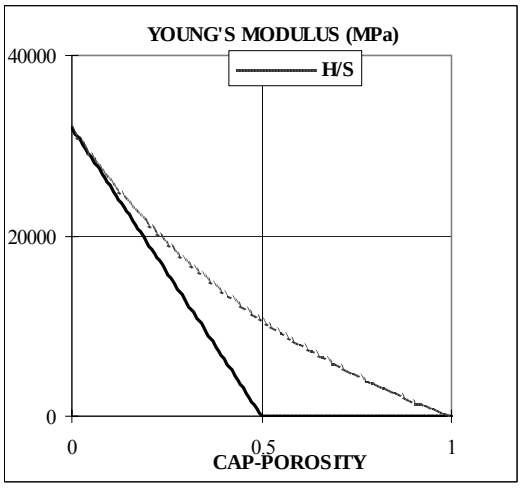


***Figure 13.*** *Cement paste system considered with other geometries than explained in the text: Solid line is geometry 1). Dashed line is geometry 2).*

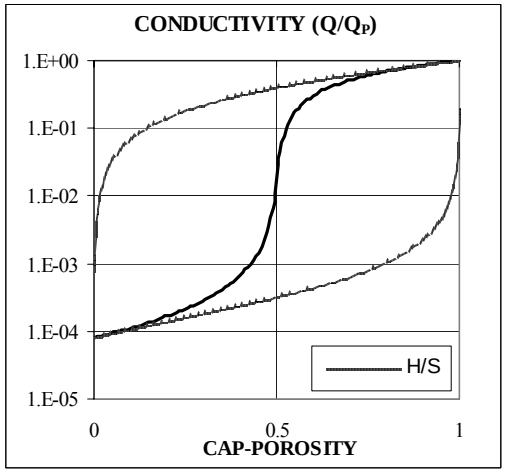


***Figure 14.*** *Cement paste system considered with other geometries than explained in the text: Solid line is geometry 1). Lower dashed line is geometry 2).*

## 5.3 Particulate composite with self-inflicted voids

Stiffness has been determined experimentally for two particulate composites with self-inflicted pores. The dotted data in Figure 15 are from tests on a cement mortar with uni-sized quartz sand (15). The dotted data shown in Figure 16 are from tests on a light clinker concrete with uni-sized compact clinkers (16). The solid lines are theoretical data reproduced from (4) where the analysis of composites with self-inflicted pores can be studied in more details.

# 6. CONCLUSION ON PROPERTY PREDICTION

The statement, that composite properties depend very much on composite geometry has been confirmed and quantified in this paper. A number of other examples, presented in the literature, also demonstrate a very satisfying agreement between theoretical predictions and experimentally obtained data (e.g. 1,17,4,18,19).

It then seems justified to state that the quality of the present theory to work with global descriptions ($\Theta$) of composite geometries qualifies it to be used in design of composite materials, meaning that the theory has the potential of predicting composite geometries which will 'produce' prescribed composite properties.

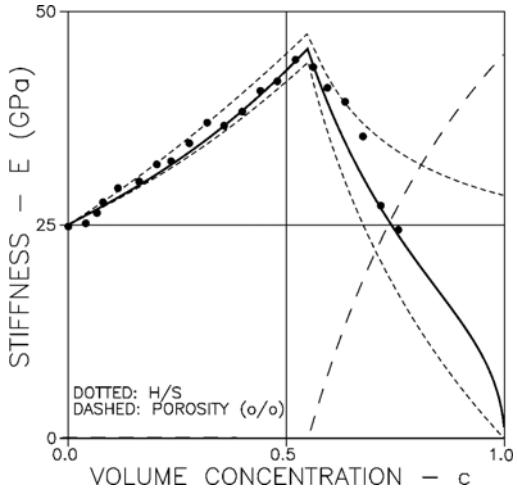


***Figure 15.*** *Stiffness of cement mortar with uni-sized quartz sand (phase P) of aspect ratios $A \approx 1$ ($\mu_P^o$,$\mu_S^o$) $\equiv$ (1,-1). Interference at $c_S \approx 0.55$. ($E_P$, $E_S$) = (75,25) GPa.*

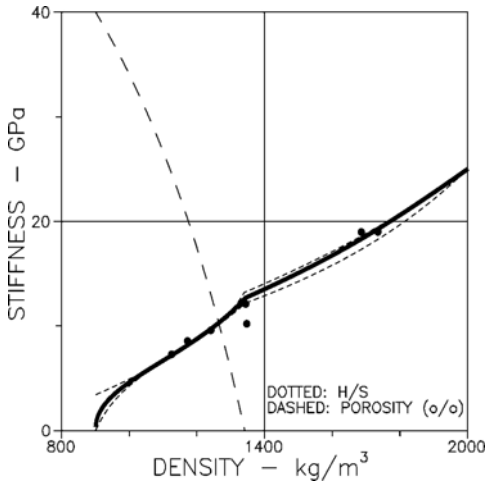


***Figure 16.*** *Stiffness of light clinker concrete with uni-sized compact clinkers (phase P) of aspect ratios $A \approx 1$ ($\mu_P^o$,$\mu_S^o$) $\equiv$ (1,-1). Interference at $c_S \approx 0.6$. ($E_P$,$E_S$) = (8,25) GPa. Densities: ($d_P$,$d_S$) = (900,2000) kg/m$^3$.*

# 7. ASPECTS OF MATERIALS DESIGN

We re-call from Section 6: The quality of the present theory to work with global descriptions ($\Theta$) of composite geometries, qualifies it to be used in design of composite materials: Predict geometry types which associate with prescribed composite properties.

We will explore this statement performing an inverse analysis of the composite expressions previously presented. Keeping our source materials defined as Phase P and Phase S, such analysis can be made by the following expressions applying for any geo-path.

## 7.1 Geo-function versus properties

The first relations who tie geometry in general ($\theta$,$\theta_Q$) and mechanical/physical composite properties (e,q) together are obtained from solving Equations 7 and 11 with respect to geo-functions. We get

$$\theta = \frac{[n - c(n-1)]e - n}{1 + c(n-1) - e} \qquad \textit{Stiffness}$$

$$\theta_Q = \frac{\left[n_Q - c(n_Q - 1\right]q - n_Q}{1 + c(n_Q - 1) - q} \qquad \textit{Conductivi ty} \tag{15}$$

## 7.2 Shape functions versus geo-functions

With known geo-functions we can now determine potential composite geometries that will "produce" prescribed composite properties. The procedure is to look at Equations 5 and 6 as shown in the following expressions 16 and 17 respectively to reveal potential geo-paths.

$$\theta = \frac{1}{2}\left[ \mu_P + n\,\mu_S + \sqrt{(\mu_P + n\,\mu_S)^2 + 4n(1 - \mu_P - \mu_S)} \right] \text{ is a root in}$$

$$\theta^2 - \theta(\mu_P + n\,\mu_S) - n(1 - \mu_P - \mu_S) = 0 \text{ relating } \mu_P \text{ and } \mu_S \text{ by} \qquad \textit{Stiffness} \quad (16)$$

$$\mu_S = \frac{n(1 - \mu_P) - \theta(\theta - \mu_P)}{n(1 - \theta)} \text{ or } \mu_P = \frac{n(1 - \mu_S) - \theta(\theta - n\,\mu_S)}{n - \theta}$$

$$\theta_Q = \mu_P + n_Q\,\mu_S + \sqrt{(\mu_P + n_Q\,\mu_S)^2 + 4n_Q(1 - \mu_P - \mu_S)} \text{ is a root in}$$

$${\theta_Q}^2 - 2\theta_Q(\mu_P + n_Q\,\mu_S) - 4n_Q(1 - \mu_P - \mu_S) = 0 \text{ relating } \mu_P \text{ and } \mu_S \text{ by} \qquad \textit{Conductivity} \quad (17)$$

$$\mu_S = \frac{4n_Q(1 - \mu_P) - \theta_Q(\theta_Q - 2\,\mu_P)}{2n_Q(2 - \theta_Q)} \text{ or } \mu_P = \frac{4n_Q(1 - \mu_S) - \theta_Q(\theta_Q - 2n_Q\,\mu_S)}{2(2n_Q - \theta_Q)}$$

## 7.3 Geo-path versus geo-functions

As previously indicated, Equations 15 – 17 apply for any geo-path, $\mu_S = f(\mu_P)$. In order to simplify matters, however, we will demonstrate the design procedure, applying the simple geo-path, $\mu_P + \mu_S = a$, previously defined in Section 3.3.1.

With a prescribed Young's modulus of E*, or conductivity Q*, at volume concentration c* the shape function values are determined as follows, meaning that *one data set* $(\mu_P^*,\mu_S^*)$ on the geo-path is determined as follows,

$$\theta^* = \frac{[n - c^*(n - 1)]\,e^* - n}{1 + c^*(n - 1) - e^*} \quad \Rightarrow$$

$$\mu_S^* = \frac{n(1 - a) + \theta^*(a - \theta^*)}{\theta^*(1 - n)} \;:\; \mu_P^* = a - \mu_S^* \qquad \textit{Stiffness} \quad (18)$$

$${\theta^*}_Q = \frac{[n_Q - c^*(n_Q - 1)]\,q^* - n_Q}{1 + c^*(n_Q - 1) - q^*} \quad \Rightarrow$$

$$\mu_S^* = \frac{4n_Q(1 - a) + {\theta^*}_Q(2a - {\theta^*}_Q)}{2\,{\theta^*}_Q(1 - n_Q)} \;:\; \mu_P^* = a - \mu_S^* \qquad \textit{Conductivity} \quad (19)$$

With two prescribed Young's moduli, $E^*_1$ and $E^*_2$, or conductivities, $Q^*_1$ and $Q^*_2$, at volume concentrations, $c^*_1$ and $c^*_2$ respectively the complete geo-path (covering any c of the composite material) can be determined utilizing that the final shape functions ($\mu_P,\mu_S$) can be determined using that shape functions vary linearly with volume concentrations as described in Section 3.3.1, (extra/interpolate linearly between ($\mu_P{}^*_1,\mu_S{}^*_1$) and ($\mu_P{}^*_2,\mu_S{}^*_2$) determined by Equations 18 and 19).

We will demonstrate this procedure in the following two examples 8.1 and 8.2 – recognizing that *prescribed properties must not – of course - violate the HS-bounds presented by Equations 12 and 13*.

**Curiosum:** We notice that Equations 18 and 19 can also be used to construct more general geo-paths than the one presently considered with a constant path factor. The equations may be used with a path factor (a) that depends on concentration (c*).

# 8. ILLUSTRATIVE EXAMPLES

## 8.1 Stiffness

The above analysis with a constant path factor is now used to determine composite geometries that will 'produce' prescribed Young's moduli from known source materials. For comparative reasons, these materials are chosen to be the same as apply in the stiffness example of Section 5.2. The results obtained are compared with predictions made with methods well known from the composite theory (Budiansky (14), Hashin (6)).

Sources: $(E_P,E_S) = (0,32000)$ Mpa (Phase P are pores)
Chosen geo-path factor: a = 0.5.
Prescribed Young's moduli: $(E^*_1,E^*_2) = (12500,5000)$ MPa at $(c^*_1,c^*_2) = (0.3,0.5)$.
Results of analysis: Figures 17 and 18.

**Remark:** The prescribed stiffness moduli above are deliberately chosen not to coincide with moduli, which can be predicted from Section 5.2. Thus, different composite geometries are looked at in the present section and Section 5.2.

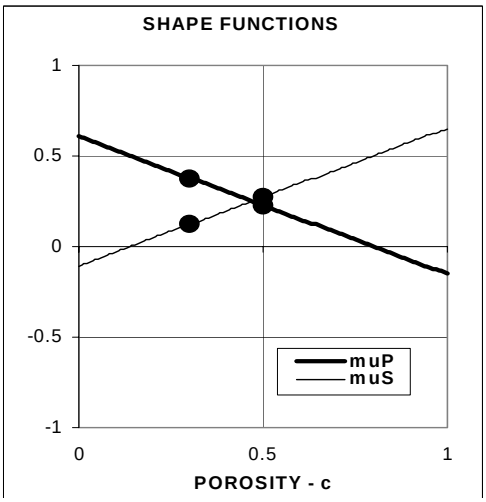


***Figure 17.*** *Shape functions of a porous material designed with a geo-path factor of 0.5 that will "produce", prescribed stiffness.*

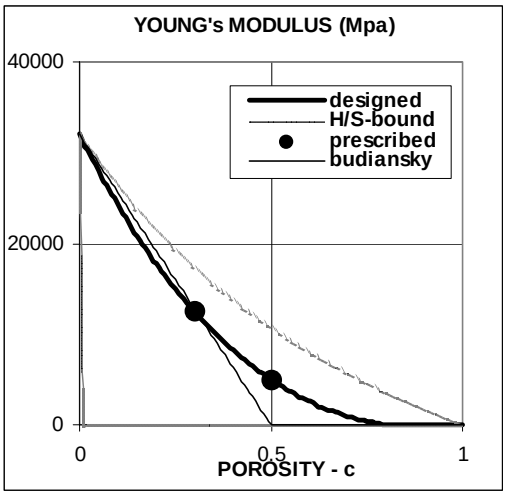


***Figure 18.*** *Stiffness of a porous material designed with a geo-path factor of 0.5 that will 'produce' prescribed stiffness.*

### Evaluation of geometry

The shape functions presented in Figure 17 are easily transformed to the geo-path graph shown in Figure 21. The prescribed stiffness data are properties of a composite produced with geometries described placing Figure 21 on top of the master path graph in Figure 5.

It can be checked by the software CompDesign previously referred to, that the shape factors ($\mu_P^o$,$\mu_S^o \approx 0.6$,-0.1) can be obtained by mixing 55% voids of aspect ratios A ≈ 20 with 45% voids of aspect ratios A ≈ 0.2.

The total geo-path in Figure 21 is based on such mixtures with critical concentrations ($c_P$,$c_S \approx 0.8$,0.14 shown in Figure 17) decided by void size distributions.

## 8.2 Conductivity

The same analysis is used in this section to determine composite geometries which will 'produce' prescribed conductivities from known source materials. For comparative reasons, these materials are chosen to be the same as apply in the diffusion example of Section 5.2. The results obtained are compared with predictions made with methods well known from the composite theory (Böttcher (20), Hashin (7)).

Sources: $(Q_P,Q_S)/Q_P = (1,0.00008)$ with $Q_P = 2*10^{-9}$ m$^2$/sec (Phase P are water saturated pores)
Chosen geo-path factor: a = 0.5.
Prescribed conductivities: $(Q^*_1,Q^*_2)/Q_P = (0.02,0.32)$ at $(c^*_1,c^*_2) = (0.29,0.55)$.
Results of analysis: Figures 19 and 20.

**Remark:** The prescribed conductivities above are deliberately chosen, not to coincide with conductivities, which can be predicted from Section 5.2. Thus, different composite geometries are looked at in the present section and Section 5.2.

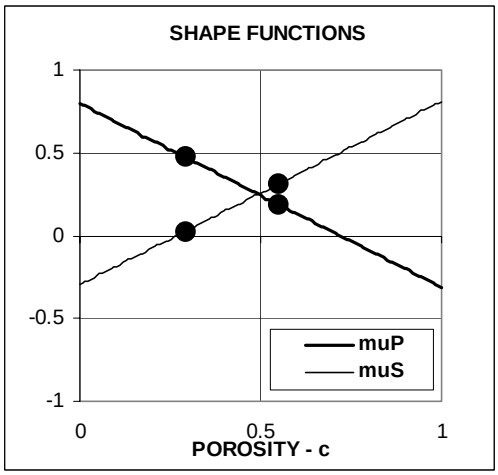


***Figure 19.*** *Shape functions of a water-saturated porous material designed with a geo-path factor of 0.5 which will "produce", prescribed conductivities.*

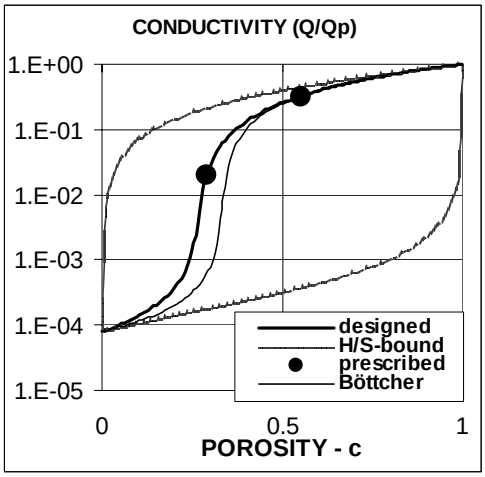


***Figure 20.*** *Conductivity of a water-saturated porous material designed with a geo-path factor of 0.5 which will 'produce' prescribed conductivities.*

### *Evaluation of geometry*

The shape functions presented in Figure 19 are easily transformed to the geo-path graph shown in Figure 22. The prescribed conductivity data are properties of a composite produced with geometries described placing Figure 22 on top of the master path graph in Figure 5.

It can be checked by the software CompDesign previously referred to that the shape factors ($\mu_P^o$,$\mu_S^o \approx 0.8$,-0.3) can be obtained by mixing 98% voids of aspect ratios A ≈ 3.6 with 2% voids of aspect ratios A ≈ 0.16.

The total geo-path in Figure 22 is based on such mixtures with critical concentrations ($c_P$,$c_S \approx 0.72,0.26$ shown in Figure 19) decided by void size distributions.

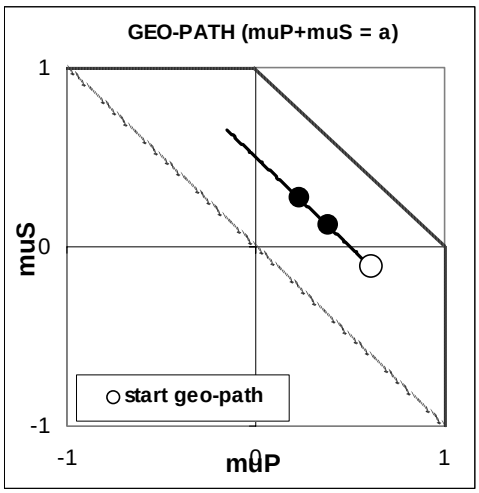


***Figure 21.*** *Geo-path in present stiffness analysis.*

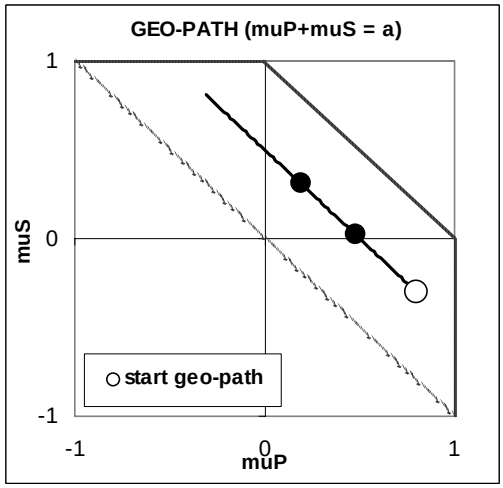


***Figure 22.*** *Geo-path in present conductivity analysis*

# 9. FUTURE RESEARCH

A method has been presented in this paper which applies for design of composites with simple geo-paths, $\mu_S + \mu_P = a$. Such geo-paths have previously been shown to apply well in property predictions for a number of composites produced with traditional technologies: Particles mixed into a continuous matrix, compaction of powders, production of porous materials, impregnation of porous materials, three dimensional 'Plywood' composites, and, see (4), particulate composites with self-inflicted pores such as light clinker concrete.

An interesting aspect of the composite theory presented in this paper is that it offers the possibility to explore in general, how geo-paths should look to obtain prescribed material properties. This feature may act as a challenge to traditional technologies: Can we do better by new, not yet known, technologies? In order to answer this question we have to open new research projects such as the following:

- FEM tests on a number of standard composites must be made - from which shape function values can be deduced at various concentrations - in principles as reported in (1,4) for various particulate composites and so-called grid composites (CC).
- Parallel technology studies must be made on, how to produce such standard composites in practice.

# 10. FINAL REMARKS

We re-call from the introductory remarks to this paper that materials are considered which exhibit linearity between response and subjected potential gradients. We emphasize that this statement means that the theory presented has a much broader field of application than indicated by the examples considered. To illustrate this feature, the results of a complex stiffness analysis made in (18) are reproduced in Figures 23 and 24. The material considered is polymer impregnated porous glass. The experiments are reported in (21). In general,

generalizations of the theory have been made in (4) which include viscoelastic composite properties. A simple version of such generalization has recently been applied by the author in (22,23,24,25) to study the rheology of extreme composites such as Self Compacting Concretes.

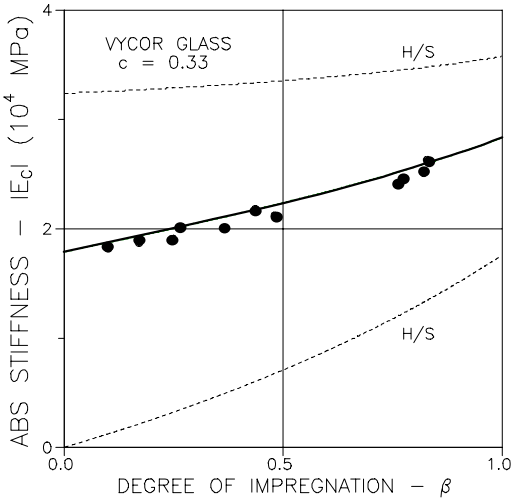


***Figure 23.*** *Absolute Young's modulus of impregnated porous glass. Dots and lines indicate experimental and predicted data respectively.*

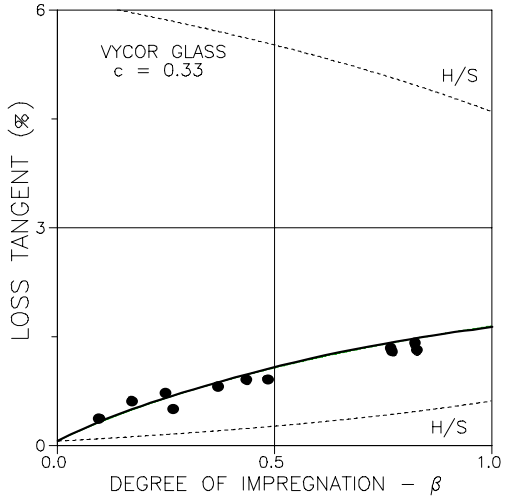


***Figure 24.*** *Loss tangent of impregnated porous glass. Dots and lines indicate experimental and predicted data respectively.*

With these remarks it seems reasonable to conclude this paper by saying that the global solutions composite theory presented in this paper might serve as a valuable 'instrument' in future materials design with respect to great many composite properties.

# 11. NOTATIONS

The symbols used in the present paper are listed below. Some symbols may deviate somewhat from those applied in (1) in which case the latter symbols are added in parenthesis. When comparing expressions in the present paper with expressions in (1) we must notice that the Poisson's parameters introduced in (1),

$$\kappa_i = 2\frac{1-2\nu_i}{1+\nu_i} \quad \gamma_i = \frac{7-5\nu_i}{2(4-5\nu_i)} \quad (i = P,S) \quad (Poisson\ parameters) \tag{20}$$

both become 1 because of the general assumption in this paper of any Poisson's ratio (ν) being 0.2.

**Abbreviations and subscripts**

| | |
|---|---|
| V | Volume |
| P | Phase P (2) |
| S | Phase S (1) |
| no subscript | Composite materials (superscript *) |
| H/S | Hashin/Shtrikman's property bounds |

**Geo-parameters**

| | |
|---|---|
| $c = V_P/(V_P+V_S)$ | Volume concentration of phase P |
| $\mu^o$ | Shape factor (ρ) |
| $\mu^1$ | Shape factor (ρ') |
| $\mu_P$ | Shape function (F) |
| $\mu_S$ | Shape function (F') |

| | |
|---|---|
| $c_P, c_S$ | Critical concentrations ($c_d, c_D$), |
| $\theta$ | Geo-function for stiffness (volumetric: $\bar{\kappa}$, deviatoric: $\bar{\gamma}$) |
| $\theta_Q$ | Geo-function for conductivity |
| $\beta$ | Degree of impregnation (vol impregnated/pore vol) |
| **Stiffness and other properties** | |
| E | Stiffness (Young's modulus) |
| $e = E/E_S$ | Relative stiffness of composite |
| $n = E_P/E_S$ | Stiffness ratio |
| Q | Conductivity (e.g. thermal, electrical, chloride) |
| $q = Q/Q_S$ | Relative conductivity of composite |
| $n_Q = Q_P/Q_S$ | Conductivity ratio |
| **Stress and strain** | |
| $\sigma$ | External mechanical stress |
| $\sigma_P$ | Phase P stress caused by external mechanical stress |
| $\sigma_S$ | Phase S stress caused by external mechanical stress |
| $\lambda$ | Linear eigenstrain (e.g. shrinkage, thermal expansion) |
| $\Delta\lambda = \lambda_P - \lambda_S$ | Linear differential eigenstrain |
| $\rho$ | Hydrostatic stress caused by eigenstrain |
| **Composite with self-inflicted voids** | |
| $(c-c_S)/c/(1-c_S)$ | Porosity of phase S for $c > c_S$ ($\equiv 0$ for $c \le c_S$) |
| $(c-c_S)/c$ | Porosity (of composite) for $c > c_S$ ($\equiv 0$ for $c \le c_S$) |
| d | Phase density |
| $d = c*d_P+(1-c)*d_S$ | Composite density |

# 12. LITERATURE


1. Nielsen, L. Fuglsang: "Elastic Properties of Two-Phase Materials", *Materials Science and Engineering, 52(1982), 39-62.*

2. *Idem:* "Shrinkage, Swelling, and Stiffness of Composites - Strain and Stress caused by hygro-thermal action and Solidification or Freezing of Liquid Imp regnant", *Bygningsstatiske Meddelelser, 62(1991), 47-78. (Published and edited by Danish Society for Structural Science and Engineering).*

3. *Idem:* "Mechanics of composite material subjected to eigenstress – with special reference to frost resistance of porous brittle material", *SBI Bulletin 96(1993), (Danish Building Research Institute).*

4. *Idem:* "Composite Materials - Mechanical and physical behaviour as influenced by phase geometry", *Monograph R-051(2003), Department of Civil Engineering, Tech. Univ. Denmark. To be downloaded from http://www.byg.dtu.dk/publicering/index_d.htm#fys*

5. Hashin, Z.: "Elastic moduli of heterogeneous materials". *J. Appl. Mech., 29 (1962), 143 - 150.*

6. Hashin, Z. and Shtrikman, S.: "Variational approach to the theory of elastic behaviour of multi-phase materials". *J. Mech. Solids, 11(1963), 127 - 140.*

7. *Idem:* "A variational approach to the theory of the effective magnetic permeability of multi-phase materials", *J. Appl. Phys. 33(1962), 3125.*

8. Larsen, E.S. and Nielsen, C.B.: "Decay of bricks due to salt", *Materials and Structures, 23(1990), 16 – 25.*

9. Beaudoin, J.J. and R.F. Feldman: "A study of mechanical properties of autoclaved Calcium silicate systems", *Cem. Concr. Res., 5(1975), 103-118.*

10. Feldman, R.F. and J.J. Beaudoin: "Studies of composites made by impregnation of porous bodies. I: Sulphur impregnant in Portland cement systems", *Cem. Concr. Res., 7(1977), 19-30.*

11. Bentz, D.P., O.M. Jensen, A.M. Coats & F.P. Glasser: "Influence of silica fume on diffusivity in cement-based materials. Part I: Experimental and computer modeling studies on cement pastes", *Cement and Concrete Research, 30(2000), 953-962.*

12. Jensen, O.M.: "Chloride ingress in cement paste and mortar measured by Electron Probe Micro Analysis", *Report R51(1998), Department of Structural Engineering and Materials, Technical University of Denmark.*

13. Nielsen, L. Fuglsang: "Strength developments in hardened cement paste – Examination of some empirical equations", *Materials and Structures, 26(1993), 255-260.*

14. Budiansky, B.: "On the elastic moduli of some heterogeneous materials", *J. Mech. Phys. Solids, 13(1965), 223 - 227.*

15. Ishai, O.: "Influence of sand concentration on deformations of mortar beams under low stresses*", ACI Journ., Proceedings 58(1961), 611-622.*

16. Palmus, L.: "Letklinkerbetons mekaniske egenskaber" (in danish, Mechanical properties of light clinker concrete), *M.Sc. thesis, Spring 1996, Dept. Struct. Engineering and Materials, Tech. Univ. Denmark.*

17. Nielsen, L. Fuglsang: "Numerical analysis of composite materials", *Materialenyt, 1(2001), DSM (Danish Society for Materials Testing and Research).*

18. *Idem:* "Elasticity and damping of porous materials and impregnated materials*", Journ. Am. Ceramic Soc., 67(1984), 93-98.*

19. *Idem:* "Strength and stiffness of porous materials*", Journ. Am. Ceramic Soc., 73(1990), 2684-89.*

20. Böttcher, C.J.F.: "The dielectric constant of crystalline powders", *Rec. Trav. Pays-Bas, 64(1945), 47.*

21. Hastrup, K.: "Polymerimpregnering af porøse materialer" (in danish, Polymer impregnation of porous materials*), Thesis, Build. Mat. Lab., Tech. Univ. Denmark, Tech. Report 42(1976).*

22. Nielsen, L. Fuglsang: "Rheology of extreme composites", *In "Papers in Structural Engineering and Materials - A Centenary Celebration", 179-187, Dept. of Struct. and Materials, Tech. Univ. Denmark, 2000.*

23. Geiker, M.R., Brandl, M., Trane, L. Nyholm, and Nielsen, L. Fuglsang: "Effect of coarse aggregate fraction and shape on the rheological properties of self-compacting concrete". *Cement, Concrete, and Aggregates, Vol. 24(2002), No. 1.*

24. Nielsen, L. Fuglsang: "Generalized Bingham description of fresh concrete", XVIII *Symposium on Nordic Concrete Research in Helsingør, Denmark, 12-14 June 2002. Proceedings, Danish Concrete Society 2002, 120-122.*

25. *Idem:* "Rheology of some fluid extreme composites - such as self-compacting concrete", *Nordic Concrete Research, 2(2001), 83-93.*